FISEVIER

Contents lists available at ScienceDirect

# Journal of Inorganic Biochemistry

journal homepage: www.elsevier.com/locate/jinorgbio



# Protein oxidation involved in Cys-Tyr post-translational modification



Susan E. Hromada<sup>1</sup>, Adam M. Hilbrands<sup>1</sup>, Elysa M. Wolf, Jackson L. Ross, Taylor R. Hegg, Andrew G. Roth, Matthew T. Hollowell, Carolyn E. Anderson, David E. Benson\*

Department of Chemistry & Biochemistry, Calvin College, Grand Rapids, MI 49546, United States

#### ARTICLE INFO

# Keywords: Protein-derived cofactors Cys-Tyr Copper-dioxygen activation Surface tyrosine oxidation Outer sphere electron transfer Native fluorescence

#### ABSTRACT

Some post-translationally modified tyrosines can perform reversible redox chemistry similar to metal cofactors. The most studied of these tyrosine modifications is the intramolecular thioether-crosslinked 3'-(S-cysteinyl)tyrosine (Cys-Tyr) in galactose oxidase. This Cu-mediated tyrosine modification in galactose oxidase involves direct electron transfer (inner-sphere) to the coordinated tyrosine. Mammalian cysteine dioxygenase enzymes also contain a Cys-Tyr that is formed, presumably, through outer-sphere electron transfer from a non-heme iron center ~6 Å away from the parent residues. An orphan protein (BF4112), amenable to UV spectroscopic characterization, has also been shown to form Cys-Tyr between Tyr 52 and Cys 98 by an adjacent Cu2+ ionloaded, mononuclear metal ion binding site. Native Cys-Tyr fluorescence under denaturing conditions provides a more robust methodology for Cys-Tyr yield determination. Cys-Tyr specificity, relative to 3,3'-dityrosine, was provided in this fluorescence assay by guanidinium chloride. Replacing Tyr 52 with Phe or the Cu<sup>2+</sup> ion with a Zn<sup>2+</sup> ion abolished Cys-Tyr formation. The Cys-Tyr fluorescence-based yields were decreased but not completely removed by surface Tyr mutations to Phe (Y4F/Y109F, 50%) and Cys 98 to Ser (25%). The small absorbance and fluorescence emission intensities for C98S BF4112 were surprising until a significantly red-shifted emission was observed. The red-shifted emission spectrum and monomer to dimer shift seen by reducing, denaturing SDS-PAGE demonstrate a surface tyrosyl radical product (dityrosine) when Cys 98 is replaced with Ser. These results demonstrate surface tyrosine oxidation in BF4112 during Cys-Tyr formation and that protein oxidation can be a significant side reaction in forming protein derived cofactors.

Tyrosine post-translational modifications able to undergo reversible oxidation provide additional reactivity beyond the canonical twenty amino acids [1-3]. Excluding topaquinone in amine oxidase [4], redoxactive tyrosine modifications/cofactors are formed by covalently crosslinking a tyrosine ring to another amino acid side chain [1,2]. Increased electron density of the phenol  $\pi$ -system by these additional functional groups or crosslinks stabilize the one-electron oxidized radical derivatives for reversible redox chemistry [5,6]. Crosslinked tyrosines include 3'-(S-cysteinyl)-tyrosine (S $\gamma$ -C $\varepsilon$ , Cys-Tyr) in galactose oxidase [7-10] and cysteine dioxygenase [11-13], 3'-(3-N-histidinyl)tyrosine (N $\varepsilon$ 2-C $\varepsilon$ , His-Tyr) in cytochrome c oxidase [14,15], 2'-(6-Nlysinyl)-topaquinone (N $\zeta$ -C $\delta$ , Lys-TOPA) in lysyl oxidase [16,17], [3'-(Smethioninyl)-5'-(6-tryptophyl)-tyrosine]  $^+$  (S $\delta$ -C $\varepsilon$ 1, C $\varepsilon$ 2-C $\zeta$ 3, Met-Tyr-Trp) [18], and the oxidation byproduct 3'-(3-tyrosine)-tyrosine ( $C\varepsilon$ - $C\varepsilon$ , dityrosine) [19]. Electron density from the thioether linkage in galactose oxidase Cys-Tyr explained how a tyrosyl radical could be stable and, along with a mononuclear copper center, participate in galactose oxidation [7]. The neutral phenol radical of His-Tyr in cytochrome c

oxidase forms due to increased stability relative to the porphyrin cation radical and attenuates the oxidative power of the most oxidized intermediate in the reaction cycle [15,20]. Prior to recognizing tyrosine post-translational modifications in galactose oxidase and cytochrome c oxidase, essential aspects of the catalytic mechanisms were under appreciated.

Despite the functional implications of redox-active tyrosine modifications, detection of these modifications is non-routine. The initial discovery of modified tyrosines used, and continues to rely on, high-resolution crystallography (< 2.4 Å resolution). Small shifts in electrophoretic mobility of the denatured state, similar to intramolecular disulfides, remain the only quantitative method in the literature for assessing the amount of Cys-Tyr crosslink formation [10,21,22]. This has hindered studies on Cys-Tyr formation and crosslinked redox-active post-translational modifications. Because Cys-Tyr is directly coordinated to a mononuclear Cu<sup>2+</sup> ion in galactose oxidase, Cys-Tyr formation was able to be explored *via* a visible absorbing chromophore [7]. These studies clearly show the need for oxidation of the precursor

<sup>\*</sup> Corresponding author at: Department of Chemistry & Biochemistry, Calvin College, 1726 Knollcrest Ave. SE, Grand Rapids, MI 49546, United States. E-mail address: dbenson@calvin.edu (D.E. Benson).

<sup>&</sup>lt;sup>1</sup> These authors contributed equally.

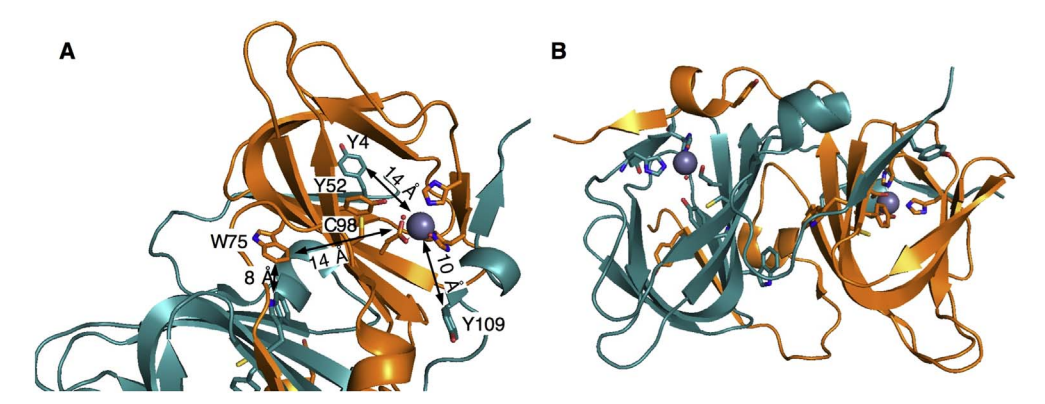


Fig. 1. Active site and surface tyrosines of the BF4112 dimer (3CEW). A) Organization of Tyr 52 (4 Å from metal ion), Tyr 4, Tyr 109, Tyr 52, Cys 98, and Trp 75 around the metal ion binding site of BF4112. B) The overall structure of the BF4112 dimer demonstrating domain swap between chains A (orange) and B (cyan). (For interpretation of the references to colour in this figure legend, the reader is referred to the web version of this article.)

tyrosine and/or cysteine side chains by the coordinated Cu<sup>+</sup> ion and dioxygen [23–25]. The gel mobility shift of denatured galactose oxidase and cysteine dioxygenase has allowed some aspects of Cys-Tyr formation to be examined [10,21]. Outer sphere tyrosine oxidation is presumed to mediate Cys-Tyr formation in cysteine dioxygenase as the percent Cys-Tyr crosslink formed increases as more cysteine is oxidized [21,26]. Dioxygenation of reduced metal ion oxidation states generates oxidizing intermediates (as in the diheme peroxidase that forms tryptophan-tryptophylquinone, TTQ, in methylamine dehydrogenase) [27]. While liquid chromatography-mass spectrometric methods have been used for crosslink identification, Cys-Tyr has significantly lower ionization yields making mass spectrometric methods difficult for yield measurement [28,29]. Mechanistic studies rely on some combination of crystallographic, absorbance change, and slight gel mobility shift to detect cofactor formation.

Due to the small size and single tryptophan, the Cys-Tyr forming orphan protein BF4112 [28] (Fig. 1) provides an excellent platform to develop an alternative assay using native fluorescence. While the highly conserved residues Tyr 52 and Cys 98 in BF4112 have been shown to form Cys-Tyr [28], variabilities in results from the gel mobility assay required an assay for robust Cys-Tyr quantitation to be developed. Here 317 nm excited, native fluorescence at pH 7 and pH 10 in 6 M guanidine are used to measure the amount of Cys-Tyr formed in BF4112. Native fluorescence was used to demonstrate the key residues important for Cys-Tyr formation in BF4112. This examination demonstrates that protein oxidation is a significant side reaction in forming these cofactors that needs to be suppressed.

## 1. Material and methods

All reagents, unless noted, were used as received from commercial vendors without further purification. Anaerobic manipulations were performed using standard Schlenk line techniques, a Coy Atmospheres anaerobic bag (Grass Lake, MI) and Teflon sealed quartz cuvettes. Two DNA plasmids were used for BF4112 expression in E. coli: one as reported previously [28] with a N-terminal YYHHHHH-tag containing two tyrosines from the His-tag along with three native tyrosines (Tyr 4, Tyr 52, Tyr 109) and one obtained from the Protein Structure Initiative (PSI from DNASU) [30] containing C-terminal HHHHH tag with three native tyrosines. Point mutations that incorporated mutations to generate Y52F, C98S, Y4F, Y109F, Y4F/Y109F, C98S/Y4F, C98S/Y109F, and C98S/Y4F/Y109F BF4112 were generated in both plasmids. All mutations generated showed pseudo-octahedral Cu2+ d-d spectra at 620 nm ( $\varepsilon \sim 5-10 \, \mathrm{M}^{-1} \, \mathrm{cm}^{-1}$ ) suggesting no changes in Cu binding to mutant BF4112 proteins. Unless otherwise noted work was performed with the PSI/DNASU construct, which has been crystallographically characterized (3CEW protein databank, PDB, accession code). Guanidine hydrochloride was purchased from Affymetrix. Dityrosine was prepared and validated by published procedures [19,31]. Methylthiocresol (4-methyl-2-methylsulfanylphenol, MTC) was synthesized

according to literature methods [32] with chloro-*tert*-butyldimethylsilane protection, ethyl acetate extraction, and deprotection to account for purification of the volatile final product.

BF4112 was prepared similarly to previously reported methods [28]. E. coli lysates containing expressed BF4112 were produced from 2 L cultures (2 × YT) that were induced with isopropyl  $\beta$ -D-1-thiogalactopyranoside (IPTG) at an optical density of 0.6, grown at 16 °C for 18 h, frozen, and passed through a French Press (10,000 psi). Lysates were clarified by centrifugation and loaded on a 5-mL immobilized metal affinity column (His-Trap, GE Healthcare) equilibrated with 50 mM tris(hydroxymethyl)aminomethane (Tris) at pH 8.0, 100 mM NaCl, and 50 mM imidazole. Undesired proteins were washed with six column volumes of loading buffer before BF4112 elution with 50 mM Tris (pH 8.0), 100 mM NaCl, 500 mM imidazole. Eluted BF4112 fractions were concentrated, reduced with 1 mM 1,4-dithiotheitol (DTT), chelated with 5 mM ethylenediaminetetraacetate (EDTA), 1 mM ophenanthroline for 4 h, and run on a size exclusion column (Superdex 200) in 50 mM Tris (pH 8.0). 100 mM NaCl. 1 mM DTT to remove metal-EDTA complexes, undesired proteins, and aggregated BF4112. BF4112 eluted at retention times consistent with a monomer (~90%, 15 kDa) and dimer. Fractions containing monomeric and dimeric BF4112 were combined, concentrated, and frozen or used. Cu2+- and Zn<sup>2+</sup>-bound BF4112 were prepared by dialysis of 100 μM metal-free BF4112 against 500  $\mu$ M Cu(NO<sub>3</sub>)<sub>2</sub> or Zn(NO<sub>3</sub>)<sub>2</sub> in 50 mM Tris (pH 8.0), 100 mM NaCl followed by dialysis (3 times) against 50 mM Tris (pH 8), 100 mM NaCl and reconcentrated. Metallated proteins were used immediately after preparation.

Cys-Tyr was formed by dithionite reduction and dioxygenation of the Cu $^2$   $^+$  center in BF4112. The buffer in concentrated protein samples (  $< 1\ mL)$  was exchanged with 50 mM 3-(N-morpholino)propane-sulfonic acid (MOPS) at pH 8.0, 100 mM NaCl using a desalting column (10-DG, Bio-Rad). Samples were reduced with 5 mM tricarbox-yethylphosphine (TCEP, Thermo) and re-run through a desalting column to remove unreacted TCEP and residual DTT. Protein samples were diluted to 100  $\mu$ M, atmosphere exchanged with nitrogen, and placed in an anaerobic bag. Protein samples were reduced with a slight excess anaerobic sodium dithionite, judged by loss of dithionite absorbance [26], and rapidly exposed to atmospheric oxygen. After Cys-Tyr chromophore was complete ( $\sim 1\ h$ ), samples were chelated with 5 mM EDTA and reduced with 1 mM DTT.

Cys-Tyr containing BF4112 samples were enriched by removing unreacted Cys 98, free thiol containing BF4112. Cysteine 98 is the only cysteine residue in BF4112, where a thiol-reactive affinity probe iodoacetyl-(PEG)2-biotin (Thermo) is added to react with any unmodified, free-thiol containing BF4112. 1 mM iodoacetyl-(PEG)2-biotin (Thermo) was added to  $100\,\mu\text{M}$  Cys-Tyr containing BF4112 sample (50 mM Tris-HCl, 5 mM EDTA, pH 8.0) and incubated in the dark for 90 min. The sample was spun down with a  $10\,\text{kDa}$  Amicon Millipore centrifuge filter to remove excess iodoacetyl-(PEG)2-biotin and resuspended in phosphate buffered saline (0.1 M phosphate, 0.15 M NaCl,

pH 7.4). The sample was added to a high capacity NeutrAvidin Agarose Resin (Thermo) column and allowed to incubate on the column for 10 min before the flow through was collected. SDS-PAGE analysis (12% gel, 5 mM DTT, samples held at 95 °C for 5 min prior to loading) confirmed removal of a weak intensity slower mobility band after treatment. Samples were deemed as 100% Cys-Tyr containing BF4112 for further analysis.

Fluorescence analysis was performed with a Fluoromax-3 (Horiba Jobin Yvon) fluorimeter with 317 nm excitation, 5 nm slit widths, 0.5 s integration time, and intensity corrected emission. Quinine sulfate (1 N H<sub>2</sub>SO<sub>4</sub>) was collected as an emission intensity standard daily for sample comparison and quantum yield calculations ( $\phi = 0.546$ ) [33]. Samples were concentrated to ~1 mM for dilution into 6 M guanidine hydrochloride, 50 mM sodium phosphate (pH 7) and 6 M guanidine hydrochloride, 50 mM sodium borate (pH 10). Protein concentrations were confirmed by Bradford assay of the concentrated stock on the day of the experiment. After background subtraction and baseline zeroing, the integrated emission intensities (counts/s) over 330 to 530 nm were collected for BF4112, MTC, and quinine sulfate samples. Spectra and integrated emission intensities were normalized to quinine sulfate emission. Spectral comparisons were also normalized to BF4112 concentration. Integrated emission intensity versus sample concentration was analyzed for pH 10 and pH 7 solutions by linear least squares for slope value and standard deviation to remove fluctuations in baseline emission. The difference in pH 10 and pH 7 slopes was used for quantum yield determination. More routine Cys-Tyr yield determinations used the ratio of pH 10 to pH 7 slopes based on a slope ratio of 2.6 found for Cys-Tyr enriched BF4112 samples.

MALDI-TOF mass spectrometry analysis of SDS-PAGE bands were performed using standard protocols. Excised gel bands were rinsed with 50% acetonitrile in 25  $\mu M$  ammonium bicarbonate, treated with DTT and iodoacetamide for alkylation and rehydrated in 25  $\mu M$  ammonium bicarbonate with mass-spec grade trypsin (1:250) and GluC (1:100) added and digested at room temperature for 24 h. Eluted digests were mixed 1:1 with a saturated  $\alpha$ -cyano-4-hydroxycinnamic acid solution containing 50% acetonitrile and 0.1% trifluoroacetic acid. Samples were spotted onto a stainless-steel plate and interrogated using a Bruker MicroFlex MALDI-TOF mass spectrometer in linear mode for increased sensitivity.

#### 2. Results

BF4112 was identified previously from a bioinformatics search of the Protein Data Bank [34] for close contacts between tyrosine and cysteine [28]. The structure of BF4112 (3CEW) was deposited by the Northeast Structural Genomics Consortium and targeted because of the novel primary sequence. Homology of the primary BF4112 sequence showed gene products from a variety of intestinal bacteria with > 60% identity with the [43] HXHKQNEEIY(52), (73) GDWLRIAPXGKR-XIXA(88) and (98)CQVK motifs highly conserved (metal ion coordinating residues underlined, Cys-Tyr residues in bold). Structure homology shows conserved cupin domain structures that contain a facial His2Glu mononuclear metal binding site, distal tyrosine, and in a couple of cases coordinated oxalate or malonate. Almost all structural homologs were from structure genomics initiatives with no documented function. No reasonable function for BF4112 can be inferred, however, there are a variety of similar bacterial proteins that could have a similar function. Even the metal ion identity is unknown as the Zn2+ ion is found in the recombinantly expressed protein that was isolated with a Zn<sup>2+</sup>-loaded metal affinity column. BF4112 loaded with a Cu<sup>2+</sup> ion, reduced anaerobically, and exposed to dioxygen (as in galactose oxidase) provided samples consistent with Cys-Tyr formation by UV absorbance, fluorescence, and proteomic mass spectrometry [28]. The single tryptophan in this protein allowed direct absorbance interrogation of Cys-Tyr formation by the absorbance at 317 nm ( $\varepsilon = 1700 \,\mathrm{M}^{-1} \,\mathrm{cm}^{-1}$ , Fig. 2A). While the physiological function of BF4112 has yet to be determined, BF4112 at the very least is a protein where Cys-Tyr formation can be further examined and assays can be developed.

Native Cys-Tyr fluorescence showed pH-dependent emission that could be used for specific quantitation. In the absence of guanidine, the 317 nm absorbance and excited fluorescence emission (Fig. 2B) were similar to dityrosine [19], except dityrosine would show protein dimerization by SDS-PAGE while Cys-Tyr would not. Denaturing conditions (6 M guanidine, 50 mM sodium borate, pH 10) provide a significant difference in emission maxima between Cys-Tyr (365-370 nm maxima, Fig. 2C) and 3.3'-dityrosine (405 nm maxima). Dityrosine emission is observed at 365 nm (borate buffer, pH 10) and 405 nm (carbonate buffer, pH 10) [19], 6 M guanidine is presumed to disrupt the borate-dityrosine interactions that lead to 365 nm emission. Emission from a model compound, MTC, in 6 M guanidine showed significant emission at pH 10 and minimal broad emission background between 350 and 400 nm at pH 7 (Fig. 2D). The lack of MTC emission at pH 7 allows background fluorescence in BF4112 from the higherquantum-yield tryptophan to be removed by subtracting pH 7 emission from pH 10 emission. Protein containing samples had variable, broad background emission at pH7 from guanidine-buffer fluorescence. Variable background fluorescence could be eliminated by determining linear regression slopes from emission spectra areas versus protein concentration plots. These slopes provided a protein concentration-independent metric of integrated emission without background fluorescence. Protein normalized emission spectra were averaged from emission spectra (baseline zeroed) with emission intensities divided by protein concentration (counts/µM·s). Despite decreased Cys-Tyr BF4112 emission intensity, the emission spectra at pH 10 and pH 7 for BF4112 and MTC (Fig. 2C,D) showed similar emission spectra. Because MTC and Cys-Tyr BF4112 have different emission intensities, emission from only Cys-Tyr in BF4112 needed to be determined. Subtraction of the pH 7 from pH 10 spectra removed BF4112 background fluorescence to provide a protein-independent quantum yield determination of (Cys-Tyr) relative to (MTC) and quinine sulfate (1 N H<sub>2</sub>SO<sub>4</sub>) for relative quantum yield determinations. Alternatively, ratio of slopes derived from pH 10 and pH 7 BF4112 titrations provided a more routine method for Cys-Tyr quantitation.

Quantum yield and pH 10/pH 7 emission ratio standards for Cys-Tyr were generated by enriching Cys-Tyr containing BF4112. Cu<sup>2+</sup>bound BF4112 was generated from E. coli expressed protein and used to produce Cys-Tyr BF4112 (see Materials and methods). Protein samples were chelated, TCEP-reduced, desalted, and reacted with an iodoacetyl-(PEG)<sub>2</sub>-biotin to modify any remaining (non-Cys-Tyr) free thiol Cys 98 residues (Fig. 3A). Biotinylated proteins were removed by passage over a high binding capacity Neutravidin-modified Sepharose resin. The resulting protein sample was used as 100% Cys-Tyr BF4112 for fluorescence standardization. Slopes of integrated emission intensity versus protein concentration were determined (Fig. 3B) and compared under the same photometric conditions to quinine sulfate and MTC standard solutions. The difference between pH 10 and pH 7 slopes provided a quantum yield of 0.062  $\pm$  0.005% for Cys-Tyr BF4112. The quantum vield is significantly smaller than that of MTC (0.45  $\pm$  0.02%). The seven-fold decrease in Cys-Tyr BF4112 quantum yield is presumably due to proton-mediated excited state quenching provided by the polypeptide backbone [35]. However, the integrated emission ratio between pH 10 and pH 7 (2.6  $\pm$  0.1) provided a robust, ratiometric method for examining Cys-Tyr yield in BF4112. Using emission ratio, factors contributing to Cys-Tyr formation in BF4112 were examined.

The necessity of Tyr 52 and Cys 98 for Cys-Tyr chromophore formation was examined using denaturing 317 nm fluorescence. Using the ratiometric method, Cys-Tyr yield was readily assessed and reliably gave 90% or higher yields (2.46  $\nu$ s 2.60, Fig. 4) if BF4112 was stored in 1 mM DTT prior to Cu<sup>2+</sup> binding and excess Cu<sup>2+</sup> was removed by dialysis followed by exchange into 50 mM MOPS (pH 8) and immediately coupled. Fluorescence yields were consistent with the

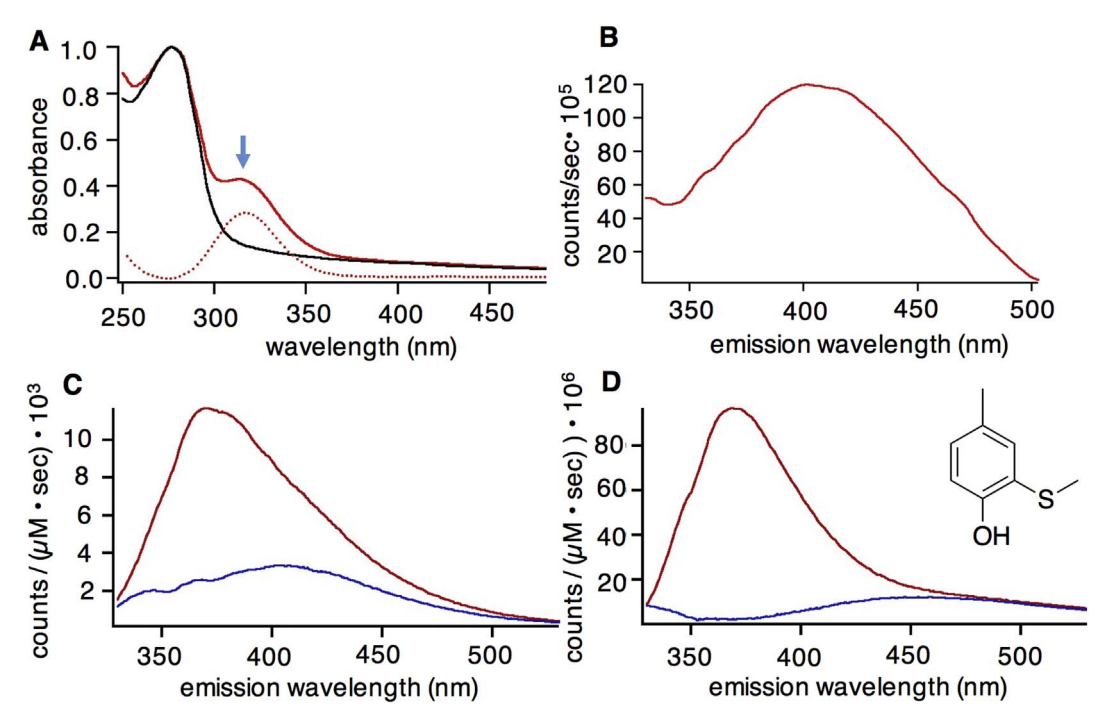


Fig. 2. Cys-Tyr BF4112 absorbance, fluorescence, and denatured fluorescence. A) absorbance before (black, bottom) and after (red, top) Cys-Tyr chromophore formation (difference spectra, dotted line). B) 317 nm excited fluorescence emission spectrum in pH 8 (50 mM MOPS, 100 mM NaCl). C) 317 nm excited fluorescence emission spectrum in 6 M guanidine hydrochloride at pH 10 (red, top) and pH 7 (blue, bottom). D) 317 nm excited fluorescence emission spectrum of MTC in 6 M guanidinium chloride at pH 10 (red, top) and pH 7 (blue, bottom). (For interpretation of the references to colour in this figure legend, the reader is referred to the web version of this article.)

magnitude of 317 nm absorbance increases in these samples. Analysis of rigorous metal-free BF4112 samples showed no fluorescence emission (0% yield). Zn<sup>2+</sup> ion-loaded BF4112 samples that were reduced and subsequently exposed to O2 reliably showed yields of 2 to 4%. Alteration of Tyr 52 to Phe also brought the yield in the range of Zn<sup>2+</sup>modified BF4112 despite lower solubility of this mutant. Altering the other two tyrosines in BF4112 to phenylalanine (Y4F/Y109F BF4112) decreased the fluorescence emission and apparent yield to 50% with an appropriate absorbance change. When Cys 98 was altered to Ser, a small 317 nm absorbance increase was observed along with a 26% yield judged by fluorescence. The fluorescence emission spectrum of the C98S BF4112 reaction product under the assay conditions was substantially different (maxima around 400 nm compared to 365 nm, Fig. 5A). In addition to the 400 nm emission, a significant shift from monomer to dimer was observed by SDS-PAGE (Fig. 5B). Performing these oxidations in Y4F, Y109F, C98S/Y4F, and C98S/Y109F BF4112 resulted in reduced solubility excluding fluorescence analysis, however the C98S/Y4F/Y109F BF4112 remained soluble and showed a small fluorescence ratio (Fig. 4). The emission spectra and SDS-PAGE analysis from C98S BF4112 are similar to what would be expected for

intermolecular dityrosine formation.

To determine the identity of sidechains causing dimerization in C98S BF4112 after oxygenation, proteomic analysis of the C98S dimer band (Fig. 5B) was performed. The dimer band of the C98S sample on the SDS-PAGE gel was excised and digested with trypsin and GluC. The complete MALDI-TOF spectrum is shown in Fig. 6. A monoisotopic peak at  $1862.1 \, m/z$  was observed (\*, Fig. 6 inset) that was consistent with a dityrosine crosslinked bis-peptide between Tyr 4 (0 missed clevages) and Tyr 109 (1C-terminal missed cleavage). A peak at this mass to charge ratio was not observed in other samples examined by proteolysis and MALDI-TOF mass spectrometry.

#### 3. Discussion

Tyr 52 and the Cu<sup>2+</sup> ion are clearly responsible for Cys-Tyr chromophore formation in BF4112. Previous mass spectrometric evidence showed a covalent linkage between Tyr 52 and Cys 98, where atomic contacts between C $\epsilon$ 2 and S $\delta$  are seen prior to Cys-Tyr identification in the crystal structure (3CEW). Since the 317 nm excited native fluorescence emission spectra in 6 M guanidine at pH 10 observed for oxidized

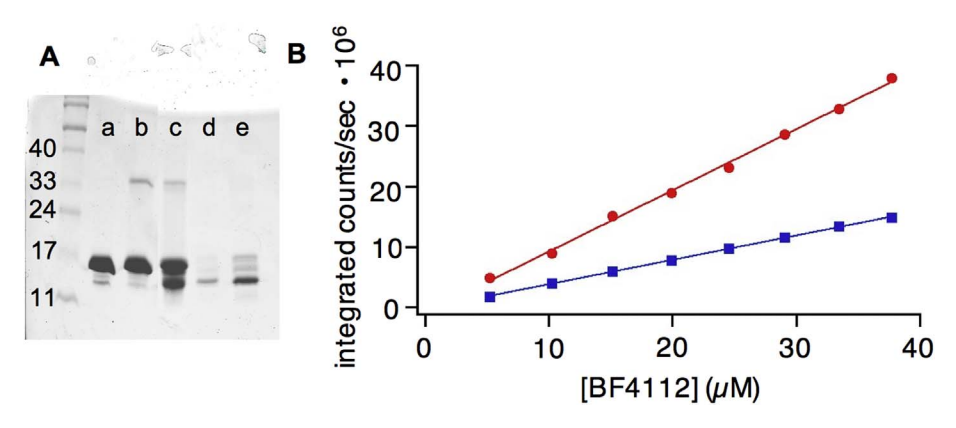


Fig. 3. Preparation and fluorescence response of enriched Cys-Tyr BF4112. A) SDS-PAGE of enriched Cys-Tyr BF4112 (10 μM): a, as purified BF4112; b, Cu²+-modified BF4112; c, non-enriched Cys-Tyr BF4112; d, iodoacetyl-(PEG)<sub>2</sub>-biotin modified samples after passage over Neutravidin column (flowthrough), e, concentrated sample in d. B) Example integrated emission area (330–530 nm) *versus* BF4112 concentration curves: red circles, pH 10; blue squares, pH 7; lines indicate linear least squares fits (pH 10,  $m=9.99\pm0.04\cdot10^5$  (integrated counts/μM BF4112), top red line; pH 10,  $m=4.06\pm0.04\cdot10^5$  (integrated counts/μM BF4112), bottom blue line). (For interpretation of the references to colour in this figure legend, the reader is referred to the web version of this article.)

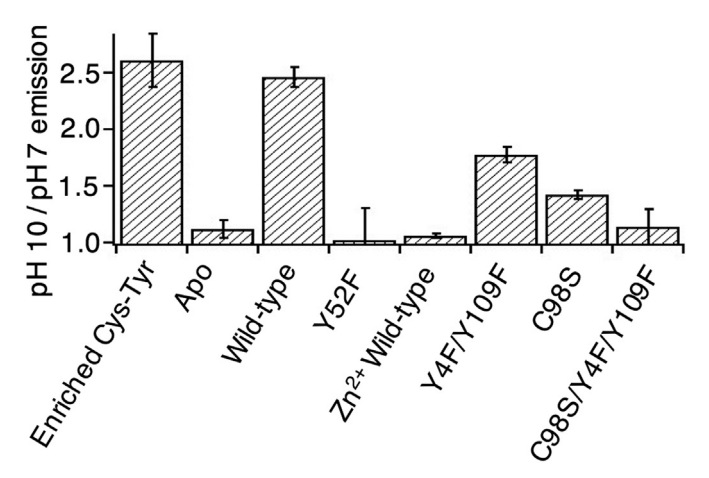
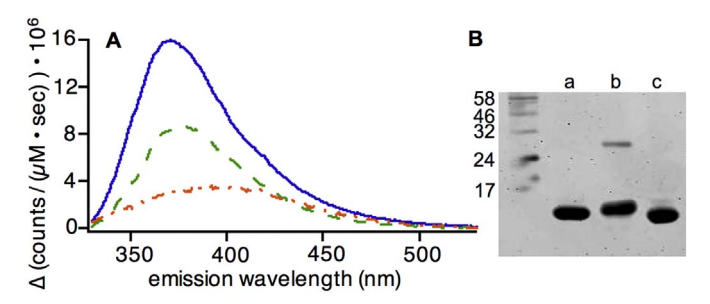
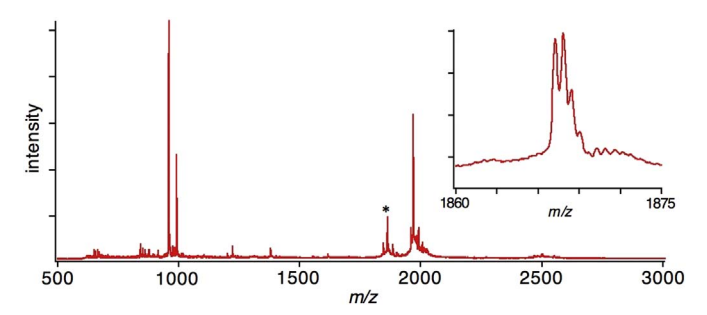


Fig. 4. Ratiometric pH emission intensity assay results that indicate Cys-Tyr yield in BF4112. Although C98S shows a significant yield, the emission spectra were red-shifted compared to all other emission spectra. Y4F, Y109F, C98S/Y4F, and C98S/Y109F were not included due to insolubility after oxidation. Error bars represent propagated standard deviations from slope determinations. (For interpretation of the references to colour in this figure legend, the reader is referred to the web version of this article.)



**Fig. 5.** Fluorescence responses and SDS-PAGE analysis of surface tyrosine mutant BF4112s. A) Difference (pH 10 minus pH 7) emission spectra (317 nm excited) in 6 M guanidinium chloride: wild-type, solid blue; Y4F/Y109F, dashed green; C98S, dash-dotted orange. Spectra were normalized to quinine sulfate emission and BF4112 concentration. B) SDS-PAGE analysis: a)  $20~\mu$ M Y4F/Y109F, b)  $20~\mu$ M C98S, and c)  $20~\mu$ M WT BF4112 after anaerobic Cu<sup>2+</sup> reduction and exposure to dioxygen. (For interpretation of the references to colour in this figure legend, the reader is referred to the web version of this article.)



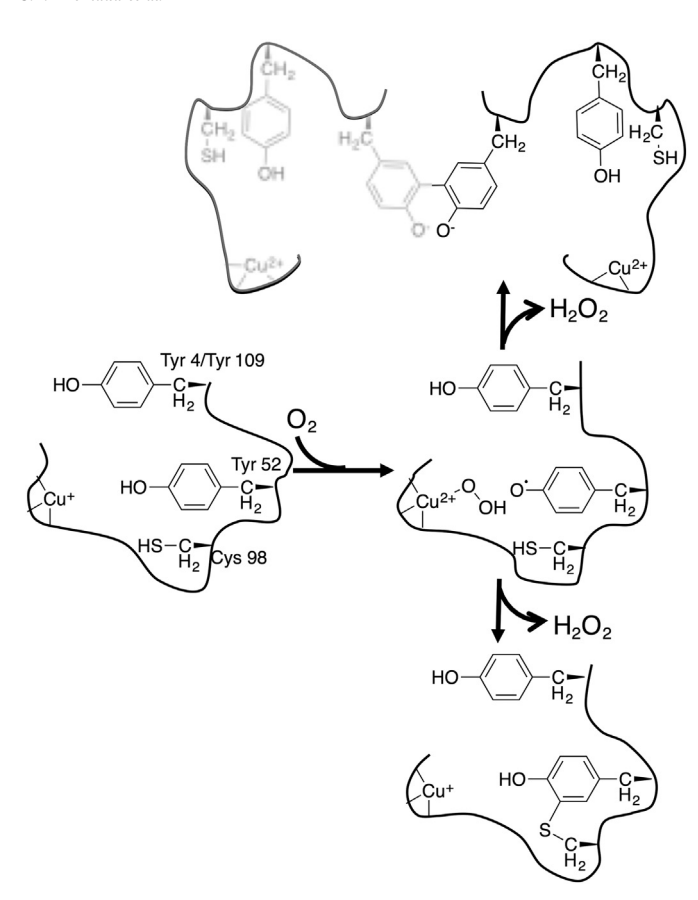
**Fig. 6.** Proteolytic digest of C98S BF4112 dimer band from SDS-PAGE. Washed/extracted sample was digested with trypsin and GluC for 24 h and placed on a stainless-steel plate for MALDI-TOF analysis: matrix,  $\alpha$ -cyano-4-hydroxycinnamic acid; linear detection mode, average of 500 shots. \* - peak of interest; inset – expansion of peak of interest, 1862.1 monoisotopic peak constaint with the  $[M+H]^+$  peak of a bis-peptide containing (3) NYQK(6) and (108)GYTMTDGGVVQLE(119), where bold letters presumably provide crosslinking.

BF4112 is consistent with MTC, the chromophore in this fluorescence analysis is highly likely to be Cys-Tyr (Fig. 2). The Cys-Tyr enrichment (Fig. 3A) provides maxima for the BF4112 Cys-Tyr quantum yield (0.046%) and pH 10 to pH 7 emission area ratio (2.60). Cys-Tyr formation yields for a variety of point mutations and conditions were examined (Fig. 4). Incorporation of Zn<sup>2+</sup> ions into the metal binding

site of BF4112 completely stops Cys-Tyr formation while the small, variable Cys-Tyr formation in "apo" BF4112 depends on the amount of adventitious redox-active metal ion incorporated into the metal binding site. The complete loss of Cys-Tyr chromophore formation for Y52F BF4112 is consistent with Tyr 52 being part of the Cys-Tyr chromophore.

Removal of two other tyrosines (Y4F/Y109F) on the surface of BF4112 decreased Cys-Tyr chromophore yield by 50%, suggesting delocalization of oxidative equivalents during Cys-Tyr formation. If Tyr 52, Cys 98, and dioxygenation of bound Cu<sup>+</sup> ion were the only necessary components for Cys-Tyr formation in BF4112, the yield for Y4F/ Y109F BF4112 would be expected to be near 100%. However, the observed 50% vield suggests additional chemistry occurs during Cvs-Tvr formation. Surface tyrosine oxidations are commonly observed in heme peroxidases and globins in the absence of substrate but presence of hydrogen peroxide [36,37]. In the formation of the tryptophan analog, TTQ, the accessory protein MauG has a group of three methionine side chains that are oxidized in the absence of substrate (pre-MADH) [38,39]. This suggests that in the absence of an appropriate pair of sidechains (Tyr 52 and Cys 98 in BF4112) for oxidative crosslinking, other protein oxidation can occur. Previous mechanistic examinations of Cys-Tyr formation in galactose oxidase suggest hydrogen atom transfer from the protonated cysteine to the  $Cu^{2+}(O_2 \cdot)^-$  moiety [23]. Tyr 52 is positioned for hydrogen atom transfer to a putative  $Cu^{2+}(O_2 \cdot)^-$  moiety, based on the 3CEW structure, forming a Cu<sup>2+</sup>(O<sub>2</sub>H)<sup>-</sup> species. The second oxidation in galactose oxidase Cys-Tyr formation is suggested to occur by Cu<sup>2+</sup>(O<sub>2</sub>H)<sup>-</sup> reduction of a Cys-Tyr transition state with a  $sp^3$  C3 of the tyrosine ring, which is then deprotonated to form Cys-Tyr [25,40]. Our best explanation is that a similar oxidation occurs through an outer-sphere process in BF4112 via a sequential two single-electron oxidation process (Scheme 1). Outersphere oxidations drive Cys-Tyr formation in cysteine dioxygenase and [11.12] Thioalkalivibrio pentaheme cytochrome c nitrite reductase [41] since no direct metal-tyrosinate coordination is observed. The observed 50% yield in Y4F/Y109F BF4112 is likely due to the monooxidized Tyr 52 radical state (Scheme 1, center) releasing superoxide rather than productively completing Cys-Tyr formation. Alternatively, long-range electron transfer from one monooxidized Tyr 52 radical site to the other monooxidized Tyr 52 radical site of the dimer would yield one site without Cys-Tyr and one site with Cys-Tyr (50%). The sequential two single-electron oxidation mechanism in Scheme 1 is also consistent with low Cys-Tyr yields observed in Tris-buffered solutions where this cationic primary amine is oxidized by any oxidized surface tyrosine, as observed previously [42,43]. Therefore, substantial delocalization of oxidative equivalents on surface tyrosines facilitate Cys-Tyr formation in BF4112.

Fluorescence emission attributed to Cys-Tyr formation in BF4112 was also, unexpectedly, observed for C98S BF4112. Given the Cys 98 involvement in Cys-Tyr, it was surprising to observe any absorbance increase of 317 nm excited fluorescence for the mutant where the thiol/ thiolate at residue 98 was altered to an alcohol. The 25% yield based on 317 nm fluorescence emission came from a different emitting species shown by the emission spectrum, where an emission maximum at 395 nm was observed rather than 365 nm as seen for all other BF4112 products and MT (Fig. 5A). Emission at 395 nm under these conditions is consistent with spectroscopic reports of dityrosine [19]. Observed 405 nm emission maximum from dityrosine samples under identical conditions confirms this conclusion, along with the observed monomerto-dimer shift in SDS-PAGE of the oxidized C98S BF4112 sample (Fig. 5B, lane b). This suggests that the 25% fluorescence yield comes from dityrosine dimerization mediated by oxidizing surface tyrosine 4 and/or 109. Mutagenesis studies showed that the C98S fluorescence response could be removed in the C98S/Y4F/Y109F BF4112 (Fig. 4), while intermediate mutant proteins were insoluble after the oxygenation step. Furthermore, MALDI-TOF analysis of the digested dimer band from the C98S BF4112 sample suggested both Tyr 4 and Tyr 109 are



**Scheme 1.** Competitive pathways for Tyrosine Post-Translational Modification. Once hydrogen abstraction of Tyr 52 occurs, electron transfer can occur within the active site (bottom) or with surface tyrosines that lead to dityrosine-mediated dimerization or interprotein electron transfer (top).

involved in the dityrosine crosslinking (Fig. 6). The small amount of dimer in lane b of Fig. 5B (~10%) is consistent with the apparent 25% yield by the fluorescence assay and dityrosine quantum yield being double the MTC quantum yield. Removal of the thiol functionality adjacent to the metal ion binding site forces, at the very least, one oxidative equivalent to a surface tyrosine to mediate radical coupling through dityrosine formation (Scheme 1). Minimal Cys-Tyr formation in the presence of Tris, but near unity conversion in the presence of MOPS, suggests surface tyrosine oxidation reversibly occurs in wildtype BF4112 as well. In the absence of Tris and presence of Cys 98 the oxidized Tyr 52 and, potentially Tyr 4 and Tyr 109, can form Cys-Tyr (Scheme 1). Thus, the surface tyrosine oxidation is a significant side reaction that needs to be suppressed in forming any redox-active tyrosine posttranslational modification. The lack of observed dityrosinedimerization in cysteine dioxygenase might be due to the monomeric nature of this protein (like myeloperoxidase vs lactoperoxidase) [44] relative to the dimerization equilibria observed with BF4112 by sizeexclusion chromatography and flexibility of tyrosines 4 and 109 at the

Cys-Tyr formation in BF4112 occurs through an outer-sphere, rather than inner-sphere, electron transfer mechanism. Cys-Tyr formation studies so far have focused on galactose oxidase, where the tyrosinate-Cu coordination mediates inner-sphere tyrosinate oxidation and hydrogen atom transfer from the thiol to a  ${\rm Cu}^{2+}({\rm O}_2 \cdot)^-$  intermediate. Inner sphere tyrosine oxidation has been shown in topaquinone formation in dopamine  $\beta$ -hydroxylase. However, many of the crosslinked protein-derived cofactors are associated but not directly coordinated to the oxidizing metal cofactors. In BF4112, outer-sphere oxidation of Cys 98 must, at least, occur while Tyr 52 oxidation through hydrogen atom transfer to  ${\rm Cu}^{2+}({\rm O}_2 \cdot)^-$ . Without tyrosinate-Cu coordination surface

tyrosine oxidation by the distal tyrosyl radical (Tyr 52 for BF4112) becomes a significant side reaction. Arrangement of protein sidechains that minimize such protein oxidation side reactions, as surface tyrosine oxidation here, are significant protein domains to be identified. For example, MauG, oxidizes a cluster of interior methionines in the absence of the TTQ forming substrate pre-MADH [38,39]. Dityrosine formation seems to be completely suppressed in mammalian cysteine dioxygenase [11,21,29], *Thioalkalivibrio* pentaheme cytochrome c nitrite reductase [45], and cytochrome c oxidase [14,15]. The mechanisms by which protein oxidation is suppressed are critically important, especially, in uncoordinated redox-active tyrosine post-translational modifications. For Cu-modified BF4112, surface tyrosine oxidation likely occurs during Cys-Tyr formation and makes dityrosine formation a significant side reaction.

#### **Abbreviations**

Cys-Tyr 3'-(S-cysteinyl)-tyrosine
His-Tyr 3'-(3-N-histidinyl)-tyrosine
TTQ tryptophan-tryptophylquinone
dityrosine 3'-(3-tyrosine)-tyrosine
MADH methylamine dehydrogenase

MauG accessory diheme peroxidase for TTQ maturation in pre-

MADH

 $\begin{tabular}{ll} MTC & 4-methyl-2-methylsulfanylphenol \\ IPTG & isopropyl $\beta$-D-1-thiogalactopyranoside \\ MOPS & 3-(N-morpholino)propanesulfonic acid \\ Tris & tris(hydroxymethyl)aminomethane \\ \end{tabular}$ 

DTT 1,4-dithiotheitol

EDTA ethylenediaminetetraacetic acid TCEP tris(2-carboxyethyl)phosphine

iodoacetyl-(PEG)<sub>2</sub>-biotin (+)-biotinyl-iodoacetamidyl-3,6-dioxaoctanediamine

## Acknowledgements

Support for this work came from National Science Foundation (CHE-1058391, and CHE-1709787, DBI-0923167, DEB; CHE-1266314, CEA), Calvin College (DEB, CEA) and Arnold and Mabel Beckman Foundation (Beckman Scholars Program, SH).

### References

- [1] V.L. Davidson, Protein-derived cofactors. Expanding the scope of post-translational modifications, Biochemistry 46 (2007) 5283–5292.
- [2] M.S. Rogers, D.M. Dooley, Posttranslationally modified tyrosines from galactose oxidase and cytochrome c oxidase, Adv. Protein Chem. 58 (2001) 387–436.
- [3] L.H. Jones, A. Narayanan, E.C. Hett, Understanding and applying tyrosine biochemical diversity, Mol. BioSyst. 10 (2014) 952–969.
- [4] J.P. Klinman, New quinocofactors in eukaryotes, J. Biol. Chem. 271 (1996) 27189–27192.
- [5] M.M. Whittaker, W.R. Duncan, J.W. Whittaker, Synthesis, structure, and properties of a model for galactose oxidase, Inorg. Chem. 35 (1996) 382–386.
- [6] K.M. McCauley, J.M. Vrtis, J. Dupont, W.A. van der Donk, Insights into the functional role of the tyrosine-histidine linkage in cytochrome c oxidase, J. Am. Chem. Soc. 122 (2000) 2403–2404.
- [7] M.M. Whittaker, V.L. DeVito, S.A. Asher, J.W. Whittaker, Resonance Raman evidence for tyrosine involvement in the radical site of galactose oxidase, J. Biol. Chem. 264 (1989) 7104–7106.
- [8] N. Ito, S.E.V. Phillips, C. Stevens, Z.B. Ogel, M.J. McPherson, J.N. Keen, K.D.S. Yadav, P.F. Knowles, Novel thioether bond revealed by a 1.7 Å Crystal structure of galactose oxidase, Nature 350 (1991) 87–90.
- [9] S.J. Firbank, M.S. Rogers, C.M. Wilmot, D.M. Dooley, M.A. Halcrow, P.F. Knowles, M.J. McPherson, S.E.V. Phillips, Crystal structure of the precursor of galactose oxidase: an unusual self-processing enzyme, Proc. Natl. Acad. Sci. 98 (2001) 12932–12937.
- [10] M.S. Rogers, A.J. Baron, M.J. McPherson, P.F. Knowles, D.M. Dooley, Galactose oxidase pro-sequence cleavage and cofactor assembly are self-processing reactions, J. Am. Chem. Soc. 122 (2000) 990–991.
- [11] C.R. Simmons, Q. Liu, Q. Huang, Q. Hao, T.P. Begley, P.A. Karplus, M.H. Stipanuk, Crystal structure of mammalian cysteine dioxygenase: a novel mononuclear iron center for cysteine thiol oxidation, J. Biol. Chem. 281 (2006) 18723–18733.

- [12] J.G. McCoy, L.J. Bailey, E. Bitto, C.A. Bingman, D.J. Aceti, B.G. Fox, G.N. Phillips, Structure and mechanism of mouse cysteine dioxygenase, Proc. Natl. Acad. Sci. 103 (2006) 3084–3089
- [13] S. Ye, X. Wu, L. Wei, D. Tang, P. Sun, M. Bartlam, Z. Rao, An insight into the mechanism of human cysteine dioxygenase. Key roles of the thioether-bonded tyrosine-cysteine cofactor, J. Biol. Chem. 282 (2007) 3391–3402.
- [14] C. Ostermeier, A. Harrenga, U. Ermler, H. Michel, Structure at 2.7 Å Resolution of the *Paracoccus denitrificans* two-subunit cytochrome c oxidase complexed with an antibody Fv fragment, Proc. Natl. Acad. Sci. 94 (1997) 10547–10553.
- [15] T.K. Das, C. Pecoraro, F.L. Tomson, R.B. Gennis, D.L. Rousseau, The post-translational modification in cytochrome c oxidase is required to establish a functional environment of the catalytic site, Biochemistry 37 (1998) 14471–14476.
- [16] S.X. Wang, M. Mure, K.F. Medzihradszky, A.L. Burlingame, D.E. Brown, D.M. Dooley, A.J. Smith, H.M. Kagan, J.P. Klinman, A crosslinked cofactor in Lysyl oxidase: redox function for amino acid side chains, Science 273 (1996) 1078–1084.
- [17] R.H. Moore, M.A. Spies, M.B. Culpepper, T. Murakawa, S. Hirota, T. Okajima, K. Tanizawa, M. Mure, Trapping of a dopaquinone intermediate in the TPQ cofactor biogenesis in a copper-containing amine oxidase from *Arthrobacter globiformis*, J. Am. Chem. Soc. 129 (2007) 11524–11534.
- [18] R.A. Ghiladi, G.M. Knudsen, K.F. Medzihradszky, P.R. Ortiz de Montellano, The met-Tyr-Trp cross-link in *Mycobacterium tuberculosis* catalase-peroxidase (KatG) autocatalytic formation and effect on enzyme catalysis and spectroscopic properties, J. Biol. Chem. 280 (2005) 22651–22663.
- [19] D.A. Malencik, J.F. Sprouse, C.A. Swanson, S.R. Anderson, Dityrosine: preparation, isolation, and analysis, Anal. Biochem. 242 (1996) 202–213.
- [20] M.R.A. Blomberg, Mechanism of oxygen reduction in cytochrome *c* oxidase and the role of the active site tyrosine, Biochemistry 55 (2016) 489–500.
- [21] E. Siakkou, M.T. Rutledge, S.M. Wilbanks, G.N.L. Jameson, Correlating crosslink formation with enzymatic activity in cysteine dioxygenase, Biochim. Biophys. Acta 1814 (2011) 2003–2009.
- [22] C.G. Davies, M. Fellner, E.P. Tchesnokov, S.M. Wilbanks, G.N.L. Jameson, The Cys-Tyr cross-link of cysteine dioxygenase changes the optimal pH of the reaction without a structural change, Biochemistry 53 (2014) 7961–7968.
- [23] M.M. Whittaker, J.W. Whittaker, Cu(I)-dependent biogenesis of the galactose oxidase redox cofactor, J. Biol. Chem. 278 (2003) 22090–22101.
- [24] M.S. Rogers, R. Hurtado-Guerrero, S.J. Firbank, M.A. Halcrow, D.M. Dooley, S.E.V. Phillips, P.F. Knowles, M.J. McPherson, Cross-link formation of the cysteine 228-tyrosine 272 catalytic cofactor of galactose oxidase does not require dioxygen, Biochemistry 47 (2008) 10428–10439.
- [25] R.E. Cowley, J. Cirera, M.F. Qayyum, D. Rokhsana, B. Hedman, K.O. Hodgson, D.M. Dooley, E.I. Solomon, Structure of the reduced copper active site in preprocessed galactose oxidase: ligand tuning for one-electron O<sub>2</sub> activation in cofactor biogenesis, J. Am. Chem. Soc. 138 (2016) 13219–13229.
- [26] J.E. Dominy, J. Hwang, S. Guo, L.L. Hirschberger, S. Zhang, M.H. Stipanuk, Synthesis of amino acid cofactor in cysteine dioxygenase is regulated by substrate and represents a novel post-translational regulation of activity, J. Biol. Chem. 283 (2008) 12188–12201
- [27] L.M.R. Jensen, R. Sanishvili, V.L. Davidson, C.M. Wilmot, In Crystallo posttranslational modification within a MauG/pre-methylamine dehydrogenase complex, Science 327 (2010) 1392–1394.
- [28] R.J. Martinie, P.I. Godakumbura, E.G. Porter, A. Divakaran, B.J. Burkhart, J.T. Wertz, D.E. Benson, Identifying proteins that can form tyrosine-cysteine

- crosslinks, Metallomics 4 (2012) 1037-1042.
- [29] T. Kleffmann, S.A.K. Jongkees, G. Fairweather, S.M. Wilbanks, G.N.L. Jameson, Mass-spectrometric characterization of two posttranslational modifications of cysteine dioxygenase, J. Biol. Inorg. Chem. 14 (2009) 913–921.
- [30] R. Xiao, S. Anderson, J. Aramini, R. Belote, W.A. Buchwald, C. Ciccosanti, K. Conover, J.K. Everett, K. Hamilton, Y.J. Huang, H. Janjua, M. Jiang, G.J. Kornhaber, D.Y. Lee, J.Y. Locke, L.-C. Ma, M. Maglaqui, L. Mao, S. Mitra, D. Patel, P. Rossi, S. Sahdev, S. Sharma, R. Shastry, G.V.T. Swapna, S.N. Tong, D. Wang, H. Wang, L. Zhao, G.T. Montelione, T.B. Acton, The high-throughput protein sample production platform of the northeast structural genomics consortium, J. Struct. Biol. 172 (2010) 21–33.
- [31] D.-I. Lee, S. Hwang, J.Y. Choi, I.-S. Ahn, C.-H. Lee, A convenient preparation of dityrosine via Mn(III)-mediated oxidation of tyrosine, Process Biochem. 43 (2008) 999–1003
- [32] I. Sylvestre, J. Wolowska, C.A. Kilner, E.J.L. McInnes, M.A. Halcrow, Copper(II) complexes of thioether-substituted salcyen and salcyan derivatives and their silver (I) adducts, Dalton Trans. (2005) 3241–3249.
- [33] D.F. Eaton, Reference materials for fluorescence measurement, Pure Appl. Chem. 60 (1988).
- [34] R.A. Laskowski, PDBsum: summaries and analyses of PDB structures, Nucleic Acids Res. 29 (2001) 221–222.
- [35] D.M. Rayner, D.T. Krajcarski, A.G. Szabo, Excited state acid-base equilibrium of tyrosine, Can. J. Chem. 56 (1978) 1238–1245.
- [36] G. Tsaprailis, A.M. English, Different pathways of radical translocation in yeast cytochrome c peroxidase and its W191F mutant on reaction with H<sub>2</sub>O<sub>2</sub> suggest an antioxidant role, J. Biol. Inorg. Chem. 8 (2003) 248–255.
- [37] C.D. Detweiler, O.M. Lardinois, L.J. Deterding, M. Ortiz, de, K.B. Tomer, R.P. Mason, Identification of the myoglobin tyrosyl radical by immuno-spin trapping and its dimerization, Free Radic. Biol. Med. 38 (2005) 969–976.
- [38] Z. Ma, H.R. Williamson, V.L. Davidson, Mechanism of protein oxidative damage that is coupled to long-range electron transfer to high-valent haems, Biochem. J. 473 (2016) 1769–1775.
- [39] E.T. Yukl, H.R. Williamson, L. Higgins, V.L. Davidson, C.M. Wilmot, Oxidative damage in MauG: implications for the control of high-valent iron species and radical propagation pathways, Biochemistry 52 (2013) 9447–9455.
- [40] D.A. Quist, D.E. Diaz, J.J. Liu, K.D. Karlin, Activation of dioxygen by copper metalloproteins and insights from model complexes. J. Biol. Inorg. Chem. (2016) 1–36.
- [41] A.A. Trofimov, K.M. Polyakov, K.M. Boiko, A.A. Filimonenkov, P.V. Dorovatovskii, T.V. Tikhonova, V.O. Popov, M.V. Koval'chuk, Structure of octaheme cytochrome c nitrite reductase from Thioalkalivibrio nitratireducens in a complex with phosphate, Crystallogr. Rep. 55 (2010) 58–64.
- [42] N.E. Good, G.D. Winget, W. Winter, T.N. Connolly, S. Izawa, R.M.M. Singh, Hydrogen ion buffers for biological research, Biochemistry 5 (1966) 467–477.
- [43] J.K. Grady, N.D. Chasteen, D.C. Harris, Radicals from "Good's" buffers, Anal. Biochem. 173 (1988) 111–115.
- [44] O.M. Lardinois, K.F. Medzihradszky, P.R. Ortiz de Montellano, Spin trapping and protein cross-linking of the Lactoperoxidase protein radical, J. Biol. Chem. 274 (1999) 35441–35448.
- [45] T. Tikhonova, A. Tikhonov, A. Trofimov, K. Polyakov, K. Boyko, E. Cherkashin, T. Rakitina, D. Sorokin, V. Popov, Comparative structural and functional analysis of two octaheme nitrite reductases from closely related Thioalkalivibrio species, FEBS J. 279 (2012) 4052–4061.